Parameter study to examine role of 3D geometric effects on bridge foundation loads resulting from demands of liquefaction-induced lateral spreading

P.S. Bhattacharjee

Department of Civil and Environmental Engineering, Washington State University, Pullman, WA, USA.

C.R. McGann

Department of Civil and Natural Resources Engineering, University of Canterbury, Christchurch.

2017 NZSEE Conference

ABSTRACT: Liquefaction-induced lateral spreading is a critical design consideration for many bridges in high-seismicity regions. Bridge foundation design procedures based on the pile pinning concept adequately account for the three-dimensionality of the problem, but do not offer much guidance on the expected significance of foundation pinning at a particular site. The purpose of this study is to quantify how changes in the 3D site geometry contribute to changes in the foundation bending demands during lateral spreading, and to identify the critical site geometric features that lead to reductions in foundation demands relative to a plane strain analysis. These objectives are accomplished using a parameter study carried out using 3D finite element models of the soil-foundation system that consider different combinations of approach embankment width, crust thickness, liquefiable layer thickness, and foundation-to-soil stiffness ratio.

1 INTRODUCTION

The response of a piled bridge foundation to the lateral deformation of the surrounding soil caused by liquefaction-induced lateral spreading depends on many different factors, including both inertial and kinematic soil-structure interaction effects. In addition to site-specific hazards and soil conditions, the design approach for such foundations should take into account the particular application for the foundations, i.e. interior piers will be handled differently than piled bridge foundations in approach embankments. For the approach embankment case, the recommended design approach for lateral spreading (Martin et al. 2002; Boulanger et al. 2006; Ashford et al. 2011) is based on the pile pinning concept, where it is assumed that the reaction forces developed in the foundations and superstructure during lateral spreading (pinning forces) can be significant relative to the driving inertial forces such that the near-field displacements are reduced. Under this approach, the design foundation displacement demand accounts for compatibility between the driving forces and the structural resistance, and is often far less than the free-field lateral spreading displacement.

Evidence of such pinning resistance has been observed at numerous bridges with approach embankments affected by lateral spreading in previous seismic events (e.g. Youd 1993; Berrill et al. 2001; Arduino et al. 2010; Wotherspoon et al. 2011), where near-field deformations are reduced significantly from the free-field soil displacement. The significance of the foundation pinning forces is driven by two 3D effects related to the finite width of the approach embankment. Firstly, the mass of soil imposing demands on the bridge foundation is limited by the width of the embankment. Secondly, because there are no lateral constraints, when liquefaction is triggered in the underlying soils the embankment soils commonly undergo large settlements and transverse deformations (perpendicular to longitudinal bridge axis), resulting in further reductions to the near-field demands. Though the pile pinning design approach is not based on a truly three-dimensional analysis, comparisons with 3D finite element analysis by McGann and Arduino (2014) have shown that the design approach recommended by Ashford et al. (2011) is consistent with a 3D description of the problem.

While the pile pinning concept is particularly attractive due to the reduction in near-field demands consistent with post-earthquake observations and 3D models, there is little information or guidance that can be used to determine how significant pinning effects may be at a given site. For example, how wide

can the embankment be relative to the bridge such that significant foundation pinning effects should be expected? Will this relationship be different for shallow versus deep liquefaction? This paper describes the results of an ongoing parameter study designed to seek answers to such questions. 3D finite element models are generated in which certain geometric properties are varied, including the embankment crest width, the thickness of the non-liquefiable crust, and the thickness of the liquefiable material. These models are analysed under loadings consistent with the kinematic demands of lateral spreading, and the effects on the embedded deep foundations are assessed. The current results of this parameter study suggest the critical importance of 3D site geometry on the response of the soil-foundation system during lateral spreading. When completed, it is expected that the results of this study will provide a first-order approximation with which to assess the relative importance of 3D effects on the bridge foundation demands due to lateral spreading at any given site.

2 3D FINITE ELEMENT MODELS

The 3D finite element models used in this study are intended to be the most simple representations of the problem that capture all of the relevant three-dimensional effects. Each model considers a single deep foundation embedded in a layered soil profile with an embankment sitting atop the upper layer. A schematic representation of the general layout used for these models is shown in Figure *1*. As shown, the generic soil profile includes a layer of saturated loose sand that is assumed to be in a fully liquefied state over the course of the analysis. No distinction is given to whether the deep foundation is a pile or drilled shaft beyond the foundation size, i.e. no installation effects are considered.

All of the models are developed and analysed using the OpenSees computational framework (McKenna 1997; McKenna et al. 2010). Solid elements are used to model the soil, beam-column elements are used to represent the deep foundation body, and the beam-solid contact element of Petek (2006) is used to represent the soil-foundation interface. The mesh for each model was generated to minimise boundary effects on the important portion of the model (soil-pile interface), and symmetry and selective mesh refinement are used as shown in Figure *1*.

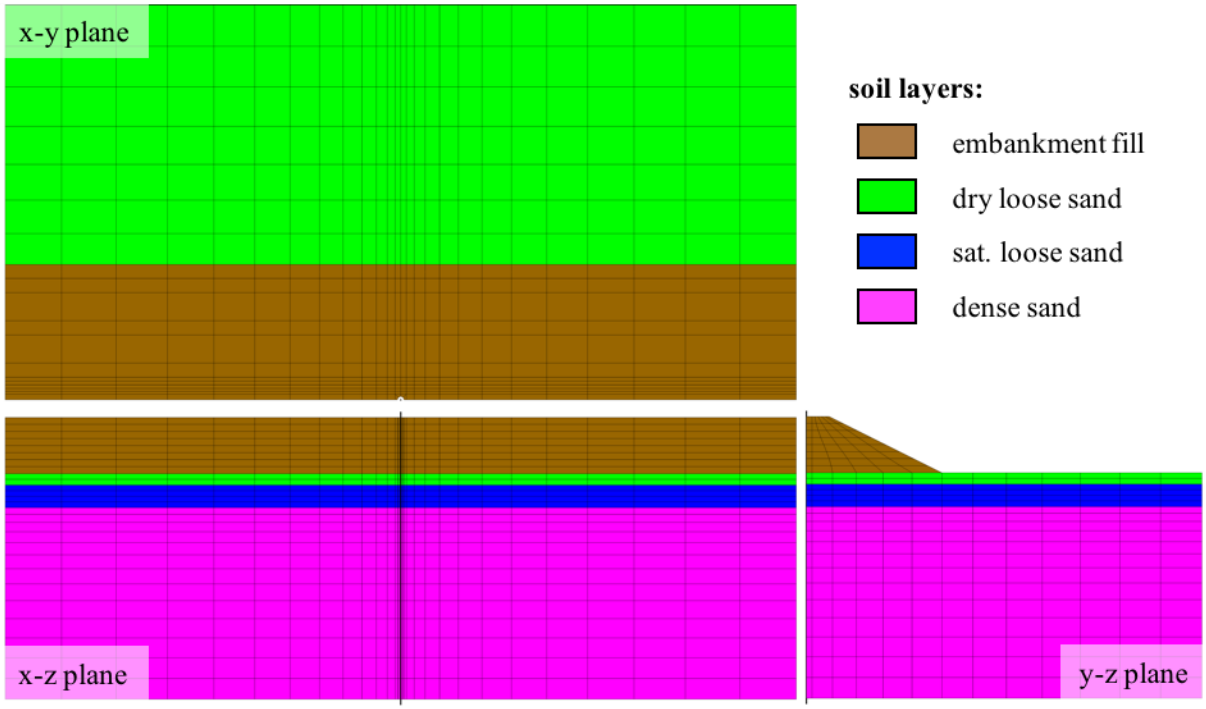

Figure 1: Typical mesh and layout for 3D finite element models used in parameter study.

2.1 Considered site geometries

The developed 3D finite element models are used to examine the effects of different site geometries on the foundation response to the demands of lateral spreading through the consideration of a large number of different geometric combinations. The geometric properties varied in these models are the

embankment crest width, the thickness of the crust layer (dry loose sand layer in Figure *1*), the thickness of the liquefiable layer (sat. loose sand layer in Figure *1*), and the diameter of the pile/shaft. The current study is an expansion of the study discussed by McGann and Arduino (2015), where 72 distinct geometric combinations were considered: three crustal thicknesses (1, 3, and 6 m); three liquefiable layer thicknesses (1, 3, and 6 m); two pile/shaft diameters (0.6 and 1.4 m); and four embankment crest widths (4, 8, 16 m and full model width).

The variations in pile/shaft diameter provide two soil-pile stiffness ratio cases, as previous work with these types of models has identified that the ratio of the soil and pile stiffness is of primary importance rather than the actual stiffness values for each (McGann et al. 2012). Figure *2* shows the four considered embankment width cases. Three of the embankment cases are representative of varying sizes of finite-width embankments for which some degree of foundation pinning is expected. These embankments are distinguished by the crest widths and are defined with 2H:1V side slopes. The fourth embankment case considers an embankment that extends across the entire model domain and for which significant foundation pinning effects are not expected. Evaluation of the degree of pinning in each of the other three cases is made relative to the results of the full width case for the same combination of pile/shaft diameter, crust thickness, and liquefiable layer thickness.

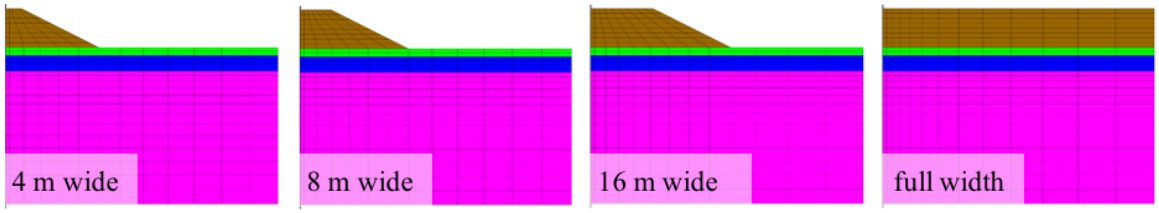

Figure 2: Embankment width cases considered in parameter study. Listed width values refer to crest width of embankments.

McGann and Arduino (2015) identified several shortcomings in the case matrix for the original parameter study, in particular with regard to the lack of more realistic crustal and liquefiable layer thickness. To expand upon this previous effort, two new crustal thicknesses (1.5 and 2 m) and two new liquefiable layer thicknesses (2 and 4 m) are added to the case matrix, resulting in a total of 200 distinct cases (72 from old study, 128 new cases). The analysis phase for these 128 new cases is currently ongoing. To date, the analyses for about 90 of these new cases have been completed, with some of the preliminary results presented in subsequent sections of this paper.

2.2 **Boundary and loading conditions**

Boundary conditions are applied only on the outer surfaces of the soil mesh, with the nodes on each surface fixed against out-of-plane translations only, and symmetry is used as shown in Figure 1. The base node of the pile is fixed against vertical translations and the upper node is fixed against all rotations to simulate the rotational fixity provided by a superstructure body. All of the pile nodes are fixed against translations out of the symmetry plane, and are only allowed rotations within the symmetry plane (i.e. out of plane and torsional rotations are fixed).

Elemental body forces equivalent to the unit weights of the various soil layers are applied to the solid elements to achieve a proper initial state of stress in the soil. A vertical force is applied to the upper pile node and held constant during the analysis to represent the self-weight of the pile and a loading from the superstructure. The kinematic demands of lateral spreading are simulated in the models by incrementally imposing displacements to the non-symmetry vertical mesh boundaries. The applied displacement profile is roughly representative of the free-field lateral spreading deformation profile, with constant displacements across the crust layer, zero displacements in the lower non-liquefiable material, and a linearly increasing profile across the liquefiable layer. The final free-field surface displacement for all of the models is 1.0 m. This approach is not able to capture effects related to pore pressure, inertia, or the initiation of liquefaction, but it is an effective way of imposing the kinematic demands of lateral spreading on the embedded foundation. Additionally, this approach enforces comparison-facilitating consistency across all of the analyses that would be difficult to achieve with dynamic effective stress analyses. Further details on the loading conditions are available in McGann and Arduino (2014,2015).

2.3 **Soil modelling**

The solid elements representing the soil layers are assigned multi-surface soil constitutive models to capture an appropriate material response. The non-liquefiable layers are represented using a pressure-dependent (Drucker-Prager type) soil constitutive model (Parra 1996; Yang 2000; Elgamal et al. 2003) with the mass density, ρ, friction angle, ϕ, and shear and bulk modulus, G_{max} and K_{max}, properties listed in Table 1. To fit within the static modelling scheme used for these models, it is assumed that liquefaction has been triggered across the entire liquefiable layer from the onset of the analysis. To this purpose, the liquefiable loose sand layer is initially defined with the residual strength and stiffness properties of a liquefied material. This layer is defined using a pressure-independent (J2 type) constitutive model (Prevost 1977) with the model properties provided in Table 1. For this modelling approach, the undrained strength, S_u, is set as the residual strength of the liquefied material. All model properties not listed in Table 1 were taken as the default values for each material model.

Table 1. Model properties for soils in 3D finite element models. Refer to Figure 1 for layer arrangement.

Layer	ρ (Mg/m^3)	ϕ (º)	G_{max} (MPa)	K_{max} (MPa)	S_u (kPa)
dry loose sand	1.7	32	75	200	–
sat. loose sand	1.7	–	6	175	5
dense sand	2.0	38	100	300	–
embankment fill	1.9	48	130	390	–

2.4 **Foundation modelling**

The foundation bodies are modelled using displacement-based beam-column elements assigned the linear elastic material and section properties listed in Table 2 (area, A, elastic modulus, E, shear modulus, G, and second area moment, I). Two circular pile/shaft models are considered, one with a 0.6 m diameter and the other with a 1.4 m diameter. For consistency with the symmetry conditions, A and I are based on half of the cross-section. Both of these foundation models are based on real template designs, and further information on these template foundations are available in McGann et al. (2012). A semi-circular space is included in the solid element mesh such that the physical size of the foundations can be considered. The beam-solid contact element of Petek (2006) is used to enforce a frictional contact condition on the surface of this empty space, linking the beam and solid nodes in a manner consistent with the kinematics of the 0.6 and 1.4 m diameter cylindrical pile/shaft bodies. The foundations are assigned a linear elastic response such that the results represent the foundation demands independent of the yield strength and plastic characteristics of the piles/shafts.

Table 2. Material and section properties for model deep foundations.

Diameter	A (m^2)	E (GPa)	G (GPa)	I (m^4)
0.6 m	0.15	31.3	12.5	0.0038
1.4 m	0.74	28.7	11.5	0.0869

3 **EFFECTS OF SITE GEOMETRY ON FOUNDATION RESPONSE**

As with the original study of McGann and Arduino (2015), the effects of variations in the geometric site parameters are primarily assessed in terms of the relative influence on the flexural response of the deep foundations as compared to the full width embankment cases. Both qualitative and quantitative assessments will be considered, though at this preliminary stage in the new expanded study, the focus is on qualitative assessment.

The results of Figure *3* demonstrate some of the qualitative observations that have been made from the completed analyses. Figure *3* shows the deformation contours in the direction of loading for all four embankment width cases corresponding to a 1.4 m diameter pile/shaft, a 1 m crustal thickness, and a 2 m thick liquefiable layer. Because the 1.4 m diameter shaft is quite stiff relative to the soil, there is little difference between the results for the 4 and 8 m wide embankments, where it is observed that the applied

free-field surface displacements of 1 m essentially exist only in the free-field (boundaries of the mesh), and the significant pinning resistance provided by the foundations is clearly evident in that the foundation displacements are about 20-25% of the free-field values. As the embankment width is increased to 16 m, the displacement of the foundation becomes larger and a smaller near-field zone of soil is affected, indicating a clear reduction in pinning resistance. In the case of the full width embankment, only minimal pinning resistance is evident, even for this stiff 1.4 m diameter shaft.

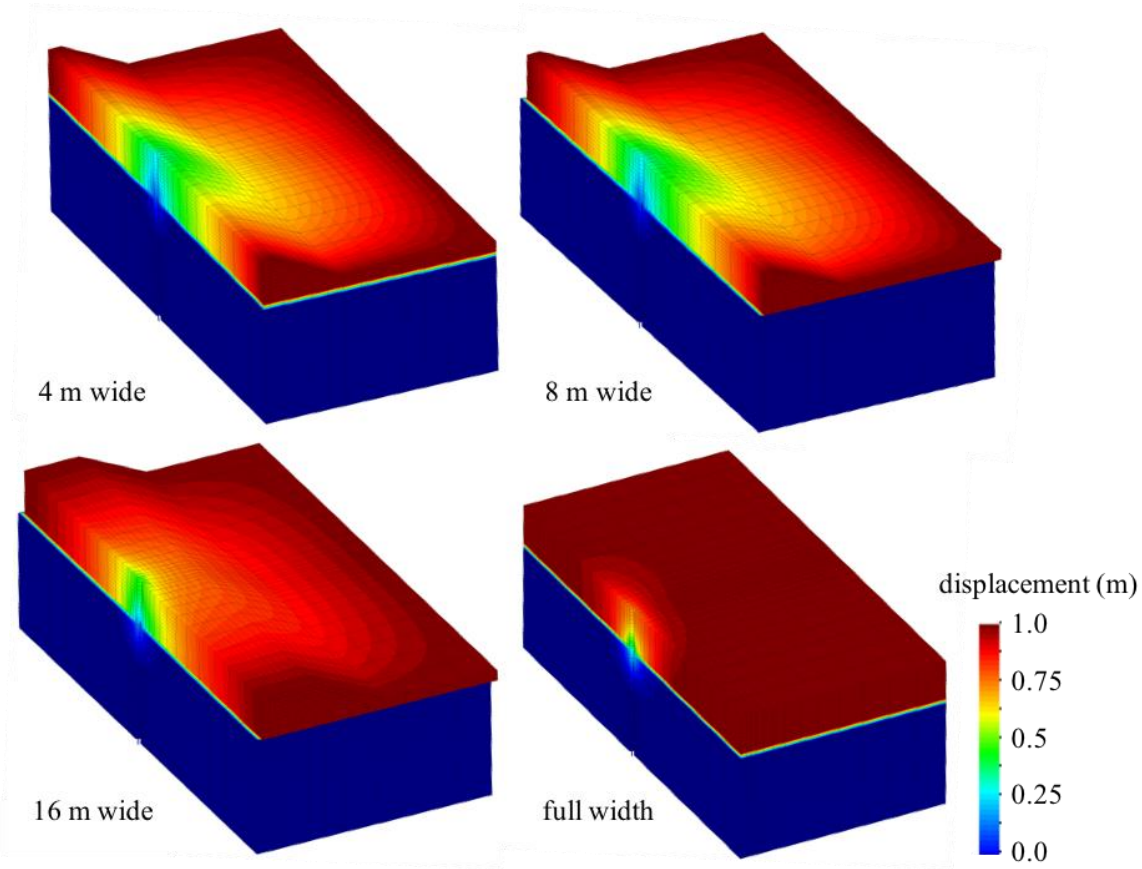

Figure 3: Contours of displacement in direction of applied lateral spreading deformation for four embankment width cases.

The thickness of the non-liquefied crust is perhaps of equal importance to the embankment width in defining the system response. Figure *4* shows the deformed shapes with contours of displacement in the direction of loading for crustal thicknesses of 1 and 3 m with a 0.6 m diameter pile, an 8 m wide embankment, and a 2 m thick liquefiable layer. As shown, the apparent pinning resistance is far greater for the shallow liquefiable layer case than for the deeper liquefiable layer, even though the embankment width is the same for both cases. For the 3 m crustal thickness, the displacement at the head of the pile is essentially identical to the free-field soil displacement. As discussed in McGann and Arduino (2015), this 3 m crustal thickness appears to be a limiting value in defining the influence of 3D embankment deformation effects in these models. For crust thicknesses < 3 m, the current results suggest that the embankment is the primary source of the kinematic demands on the foundation, and thus changes in embankment width affect significant changes in response. For crust thicknesses ≥ 3 m, the crustal material itself is the primary source of kinematic demands. The 1.5 and 2 m crustal thicknesses cases considered in the expansion of the parameter study were selected to explore this effect further.

The ratio of the foundation bending stiffness relative to the stiffness of the soil also plays a relatively intuitive role in defining the system response. With everything else equal, the deformation of the 0.6 m diameter case is larger than the corresponding 1.4 m diameter model, and changes in system response are affected for narrower embankments and shallower crustal thicknesses. For example, in the 0.6 m diameter cases corresponding to the results of Figure *3*, there is a discernible difference between the 4 and 8 m wide embankment cases, while these two cases are negligibly different for the 1.4 m shaft.

These observations make intuitive sense, as increasing the size or stiffness of the foundation is a natural way to reduce the structural displacements resulting from lateral spreading, and it is encouraging that the model results and trends correspond to expected behaviours. The thickness of the liquefiable layer has the most subtle effect on the foundation bending demands of the considered geometric properties. There are differences observed as this parameter is varied, particularly in regard to the foundation shear forces, but no clear trend that holds across all of the cases has yet emerged.

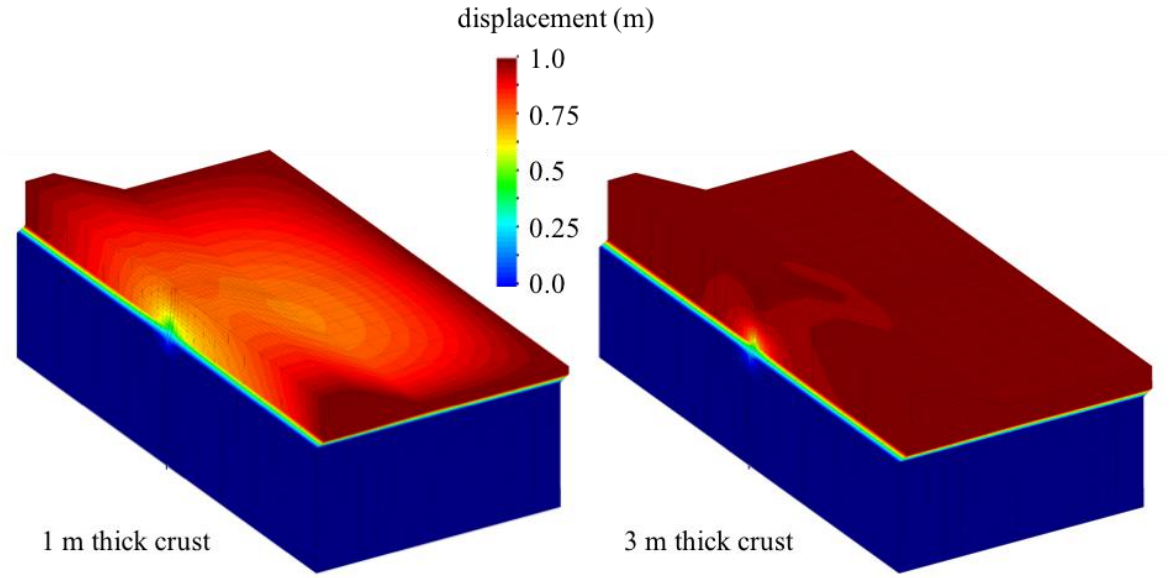

Figure 4: Contours of displacement in direction of applied lateral spreading deformation for two crust thickness cases.

4 CONCLUSIONS

Foundation pinning is an important consideration in the design of piled bridge foundations to withstand liquefaction-induced lateral spreading. Current design procedures for this case that account for pinning resistance (Martin et al. 2002; Boulanger et al. 2006; Ashford et al. 2011) have been shown to produce results consistent with a fully three-dimensional representation of the problem, however, there is a general lack of information regarding how significant pinning effects should be for a given site. To address this issue, a parameter study investigating the differences in foundation bending demands across variations in different site geometric properties is being carried out using 3D finite element analyses. This current study expands the case matrix originally considered by McGann and Arduino (2015) from 72 to 160 distinct cases, with an emphasis on more realistic configurations rather than the broader, more enveloping range of values represented in the original case matrix.

The results to date indicate the general significance of the geometric aspects of each site on the bending demands developed in the deep foundations due to the kinematic demands of lateral spreading. The near-field alteration of the soil deformation caused by foundation pinning varies greatly with changes geometric properties such as the embankment width, where less resistance is observed for increasing width of embankment, and the thickness of the non-liquefied crust in the soil profile. Once the expanded parameter study is completed, the goal is to produce a simple equation through analysis of the aggregate foundation flexural demands that allows for an estimation of the expected significance of pinning effects given the particular combination of embankment width, crustal thickness, liquefiable layer thickness, and soil-foundation stiffness ratio at any given site. The significance of the pinning effects will be framed in terms of the ratio between the flexural demands in a given case to those in the corresponding full width embankment case, such that a low ratio indicates that pinning effects are significant, a higher ratio indicates that pinning effects are less significant, and a ratio of 1.0 indicates no pinning resistance (i.e. same demands as full width case). It is also anticipated that further cases will be added to the parameter matrix to consider further variations to the currently-considered geometric properties (in particular an embankment width > 16 m) as well as changes to other aspects of the models not currently being varied, such as the soil properties and embankment height.

5 ACKNOWLEDGEMENTS

Financial support for this research was provided by the Pacific Northwest Transportation Consortium (PacTrans). This project was also partially supported by QuakeCoRE, a New Zealand Tertiary Education Commission-funded Centre. This is QuakeCoRE publication number 0135.

6 REFERENCES

Arduino, P., Ashford, S.A., Assimaki, D.A., Bray, J.D., Eldridge, T., Frost, D., Hashash, Y., Hutchinson, T. & Johnson, L., et al. (2010). *Geo-engineering Reconnaissance of the 2010 Maule, Chile Earthquake.* In J.D. Bray and D. Frost (ed), Report No. GEER-022, Geo-Engineering Extreme Events Reconnaissance (GEER) Association.

Ashford, S.A., Boulanger, R.W. & Brandenberg, S.J. (2011). *Recommended Design Practice for Pile Foundations in Laterally Spreading Ground*. PEER Report No. 2011/04. Pacific Earthquake Engineering Research Center, University of California, Berkeley.

Berrill, J.B., Christensen, S.A., Keenan, R.P., Okada, W. & Pettinga, J.R. (2001). Case study of lateral spreading forces on a piled foundation. *Géotechnique*, 51(6): 501-517.

Boulanger, R.W., Chang, D., Gulerce, U., Brandenberg, S.J. & Kutter, B.L. (2006). Evaluating pile pinning effects on abutments over liquefied ground. In: R.W. Boulanger & K. Tokimatsu (ed), *Seismic Performance and Simulation of Pile Foundations in Liquefied and Laterally Spreading Ground.* ASCE GSP 145: 306-318.

Elgamal, A., Yang, Z., Parra, E. & Ragheb, A. (2003). Modeling of cyclic mobility in saturated cohesionless soils. *International Journal of Plasticity*, 19: 883–905.

Martin, G.R., March, M.L., Anderson, D.G., Mayes, R.L. & Power, M.S. (2002). Recommended design approach for liquefaction induced lateral spreads. In: *Proc., 3rd Natl. Seismic Conf. and Workshop on Bridges and Highways.* MCEER-02-SP04, Buffalo, NY.

McGann, C.R. & Arduino, P. (2014). Numerical assessment of three-dimensional foundation pinning effects during lateral spreading at the Mataquito River Bridge, *Journal of Geotechnical and Geoenvironmental Engineering*, 140(8): 04014037.

McGann, C.R. & Arduino, P. (2015). Numerical assessment of the influence of foundation pinning, deck resistance, and 3D site geometry on the response of bridge foundations to demands of liquefaction-induced lateral soil deformation, *Soil Dynamics and Earthquake Engineering*, 79: 379-390.

McGann, C.R., Arduino, P. & Mackenzie-Helnwein, P. (2012). *Development of Simplified Analysis Procedure for Piles in Laterally Spreading Layered Soils.* PEER Report No. 2012/05: Pacific Earthquake Engineering Research Center, University of California, Berkeley.

McKenna, F.T. (1997). *Object-Oriented Finite Element Programming: Frameworks for Analysis, Algorithms and Parallel Computing*. Ph.D. Dissertation, University of California, Berkeley.

McKenna, F.T., Scott, M.H. & Fenves, G.L. (2010). Nonlinear finite element analysis software architecture using object composition. *Journal of Computing in Civil Engineering*, 24(1): 95-107.

OpenSees. (2007). Open System for Earthquake Engineering Simulation. http://opensees.berkeley.edu; University of California, Berkeley: Pacific Earthquake Engineering Research Center (PEER).

Parra, E. (1996). *Numerical Modeling of Liquefaction and Lateral Ground Deformation Including Cyclic Mobility and Dilation Response in Soil System*. Ph.D. Dissertation, Rensselaer Polytechnic Institute, Troy, NY.

Petek, K.A. (2006). *Development and Application of Mixed Beam-Solid Models for Analysis of Soil-Pile Interaction Problems*. Ph.D. Dissertation, University of Washington.

Prevost, J.H. (1977). Mathematical modeling of monotonic and cyclic undrained clay behavior. *International Journal for Numerical and Analytical Methods in Geomechanics*, 1: 195-216.

Wotherspoon, L.M., Bradshaw, A., Green, R., Wood, C., Palermo, A., Cubrinovski, M. & Bradley, B.A. (2011). Performance of bridges during the 2010 Darfield and 2011 Christchurch earthquakes. *Seismological Research Letters*, 82(6): 950-964.

Yang, Z. (2000). *Numerical Modeling of Earthquake Site Response Including Dilation and Liquefaction*. Ph.D. Dissertation , Columbia University, New York.

Youd, T.L. (1993). Liquefaction-induced damage to bridges. *Transportation Research Record: Journal of the Transportation Research Board No. 1411*: 35-41.